

Wavefront sensing, novel lower degree/higher degree polynomial decomposition and its recent clinical applications: A review

Radhika Rampat, Jacques Malet, Laurent Dumas¹, Damien Gatinel

We are in the midst of a shift towards using novel polynomials to decompose wavefront aberrations in a more ophthalmologically relevant way. Zernike polynomials have useful mathematical properties but fail to provide clinically relevant wavefront interpretation and predictions. We compared the distribution of the eye's aberrations and demonstrate some clinical applications of this using case studies comparing the results produced by the Zernike decomposition and evaluating them against the lower degree/higher degree (LD/HD) polynomial decomposition basis which clearly dissociates the higher and lower aberrations. In addition, innovative applications validate the LD/HD polynomial basis. Absence of artificial reduction of some higher order aberrations coefficients lead to a more realistic analysis. Here we summarize how wavefront analysis has evolved and demonstrate some of its new clinical applications.

Key words: LD/HD polynomial, wavefront aberrometry, zernike polynomials

In recent decades, advances in refractive surgical techniques and tools have progressed hand in hand with a need for accurate analysis of the corneal surface and ocular aberrations.^[1] These aberrations can be chromatic or monochromatic, with monochromatic aberrations divided into higher and lower order. Lower (second) order aberrations include positive defocus (myopia), negative defocus (hyperopia), and regular astigmatism. Higher order aberrations can induce bothersome visual symptoms such as glare, halos, starbursts and ghost images. Hartmann and Tschernig pioneered work in the nineteenth century and allowed analysis of these aberrations which signify a deviation from the ideal optical system.^[2] Indeed the principles of aberrometry are broadly based on the study of the excursions of the reflected wave compared to a reference aberration-free wave.^[3] Many types of aberrometers exist to measure these aberrations.^[4,5] Inter-aberrometer disagreements seemed to occur mostly in the higher order aberrations (HOAs): lower order depending on sensor type and higher order on the type of expansion used.^[6-8] Analysis of wavefront aberrations involves splitting them into multiple components and using mathematical equations to define them.^[9] The data is most conveniently expressed in polynomial form with several decomposition methods trialed previously including Fourier series and Zernike polynomials.^[10,11] Such approach incurs the breakdown of the wavefront error into components that visually and mathematically describe distinct elements of the overall aberration. The magnitude of total aberrations is computed as a Root Mean Square (RMS) coefficient. In addition to the determination of objective refraction via the computation of low order coefficients, the benefits of such an approach is to quantify and qualify individual higher order aberrations

Rothschild Foundation Hospital, Paris, France, ¹Mathematics Laboratory of Versailles, UVSQ, CNRS, Université Paris-Saclay, Versailles, France

Correspondence to: Dr. Damien Gatinel, Fondation Ophtalmologique Rothschild, 29 Rue Manin, Paris, France. E-mail: gatinel@gmail.com

Received: 01-Jun-2020

Revision: 17-Aug-2020

Accepted: 27-Aug-2020

Published: 23-Nov-2020

Access this article online

Website:

www.ijo.in

DOI:

10.4103/ijo.IJO_1760_20

Quick Response Code:



which were inseparable before and termed generically as “irregular astigmatism”. Computational and adaptive optics allow one to explore the contribution of corrected aberrations, beyond spectacle correction, to the visual performance.^[12-14] Detecting ectasia was a particular sub-field of interest due to its impact on refractive surgery outcomes in those individuals with keratoconus.^[15-17] A clinically relevant analytical method is required for custom photoablation programming intended to safely and accurately correct or modify sphero-cylindrical refractive error and high degree aberrations.

In this review, we present the first study of the distribution of the coefficients assigned to the LD/HD polynomials for unoperated ametropic eyes, for eyes operated by refractive surgery and eyes affected by keratoconus. Examples as well as a non-exhaustive list of potential applications will be presented to illustrate the differences between the decomposition into Zernike polynomials and the LD/HD method.

Background

Zernike polynomials

Each polynomial relays a mathematical wavefront appearance, and the linked coefficient assigns weight to that particular aberration within the total wavefront map. Zernike coefficients are labelled with a double-indexing scheme corresponding with the standard labelling notation established by the Vision Science and Its Applications Standards Taskforce team.^[18]

This is an open access journal, and articles are distributed under the terms of the Creative Commons Attribution-NonCommercial-ShareAlike 4.0 License, which allows others to remix, tweak, and build upon the work non-commercially, as long as appropriate credit is given and the new creations are licensed under the identical terms.

For reprints contact: WKHLRPMedknow_reprints@wolterskluwer.com

Cite this article as: Rampat R, Malet J, Dumas L, Gatinel D. Wavefront sensing, novel lower degree/higher degree polynomial decomposition and its recent clinical applications: A review. Indian J Ophthalmol 2020;68:2670-8.

Until recently, Zernike polynomials were the gold standard for analyzing wavefront aberrations, the modes depicted in a pyramid formation.^[18,19] Though their orthonormality over a round pupil lent themselves to solving some of the mathematical issues allowing calculation of the total magnitude in the form of a root mean square (microns), they had some shortcomings summarized elsewhere.^[10,20-22]

There are an unlimited number of Zernike polynomials, though for clinical relevance the decomposition of the wavefront is limited to the first twenty-eight Zernike modes with a maximal order of 6. The top three rows are part of the lower order aberrations (LOAs) with the highest value of the radial term being two. This radial order of a mode is the highest but may contain others within its analytical expression. For example, a mode of order (n) could contain low order terms such as r^{n-2} or r^{n-4} . The central five columns contain modes which have low order terms to ensure it is orthogonal with the lower radial degree modes but same azimuthal frequency. Therefore, higher degree spherical aberration modes such as Z_4^0 and Z_6^0 contain some radial terms r^2 which denotes defocus. In summary, low order terms such as tilt and defocus are contained in the analytical expressions of a few high order modes. This ineffective separation between low and higher order wavefront error would be likely to cause imprecise estimation of subjective refraction as well as point spread functions of higher order aberrations (HO-PSF) whereby convolutional techniques could project an anticipated retinal image.^[23]

New Polynomials and LD/HD (Low Degree/High Degree) basis

Proper separation of the wavefront into lower and higher order components is crucial in several clinical tasks. In order to get a more clinically realistic picture of ocular aberrations, a novel polynomial basis aimed at providing a clear cut between low degree (LD) and high degree (HD) wavefront errors was proposed recently. The new LD/HD polynomials decomposition basis was described^[24,25] and demonstrated with clinical examples^[22] in articles published in 2018 and 2020 respectively.

The modes are still arranged in a pyramid [Fig. 1] with a double index format $G(n,m)$ where n and m have the same meaning, as in the Zernike classification, with the new higher order $G(n,m)$ modes located in the five central columns being devoid of lower order terms [Table 1, end of document]. The absence of a low degree term in these high degree modes of the LD/HD classification is responsible for a simplification of the geometry of the wavefront error that they characterize with respect to the corresponding Zernike modes [Fig. 2a]. Their profile is flatter in the paracentral region [Fig. 2b], suggesting less interaction with sphero-cylindrical refraction. The analytical structure of these modes being homogenized, may improve the relevance of the comparison between the coefficients which weight them. The acquisition of a new wavefront measurement with the aberrometer is not necessary, as the coefficients weighting the new polynomials can be directly computed analytically from the coefficients weighting a Zernike expansion for the same fit order. Just like the Zernike coefficient, the LD/HD coefficient also changes with pupil size. To achieve proposed separation between the low order and higher order wavefront errors, the notion of orthogonality was rejected between higher and lower order but not within. Therefore, the total RMS cannot be calculated directly from the low RMS and high RMS values using Pythagorean calculations. It is however possible to calculate RMS coefficients of grouped modes within the low (LD component) and within the high order (HD component) modes.

Table 1: Comparison of the Analytical Expression in Polar Coordinates of the New Higher Order $G(n, m)$ and Their corresponding Zernike Modes Up to the 6th Radial Order on a Unit Circular Pupil Domain of Radius r and Polar Angle θ

Z_3^{-1}	$= 2\sqrt{2}(3r^3 - 2r) \sin(\theta)$
G_3^{-1}	$= 2\sqrt{2} r^3 \sin(\theta)$
Z_3^{+1}	$= 2\sqrt{2}(3r^3 - 2r) \cos(\theta)$
G_3^{+1}	$= 2\sqrt{2} r^3 \cos(\theta)$
Z_4^{-2}	$= \sqrt{10}(4r^4 - 3r^2) \sin(2\theta)$
G_4^{-2}	$= \sqrt{10} r^4 \sin(2\theta)$
Z_4^0	$= \sqrt{5}(6r^4 - 6r^2 + 1)$
G_4^0	$= \sqrt{5}r^4$
Z_4^{+2}	$= \sqrt{10}(4r^4 - 3r^2) \cos(2\theta)$
G_4^{+2}	$= \sqrt{10} r^4 \cos(2\theta)$
Z_5^{-1}	$= 2\sqrt{3}(10r^5 - 12r^3 + 3r) \sin(\theta)$
G_5^{-1}	$= 2\sqrt{3}(5r^5 - 4r^3) \sin(\theta)$
Z_5^{+1}	$= 2\sqrt{3}(10r^5 - 12r^3 + 3r) \cos(\theta)$
G_5^{+1}	$= 2\sqrt{3}(5r^5 - 4r^3) \cos(\theta)$
Z_6^{-2}	$= \sqrt{14}(15r^6 - 20r^4 + 6r^2) \sin(2\theta)$
G_6^{-2}	$= \sqrt{14}(6r^6 - 5r^4) \sin(2\theta)$
Z_6^0	$= \sqrt{7}(20r^6 - 30r^4 + 12r^2 - 1)$
G_6^0	$= \sqrt{7}(6r^6 - 5r^4)$
Z_6^{+2}	$= \sqrt{14}(15r^6 - 20r^4 + 6r^2) \cos(2\theta)$
G_6^{+2}	$= \sqrt{14}(6r^6 - 5r^4) \cos(2\theta)$

Three clinical vignettes below demonstrate the clinical importance of utilizing LD/HD rather than Zernike polynomials. This study was approved by the Institutional Review Board at Rothschild foundation and followed the tenets of the Declaration of Helsinki. Informed consent was obtained from all participants.

Distribution of the LD/HD Wavefront Coefficients to Describe the Eye's Wavefront Aberrations

The OPD-Scan aberrometer is a combined wavefront aberrometer and Placido-disk topographer. The measurement details have been previously described.^[26,27]

Our normal population consisted of 220 normal subjects seeking assessment for refractive surgery, each having a spherical refraction between -11.50 D and +4.50 D and a refractive astigmatism of less than 3.00 D. One eye was randomly selected from each patient for analysis. 114 eyes from 114 patients routinely followed up for keratoconus who never had any corneal surgery, were also analyzed. In addition, 165 eyes of 165 patients operated with uncomplicated LASIK were also analyzed.

All OPD-Scan measurements were acquired in a dark examination room after 2 minutes of dark adaptation and were

repeated three consecutive times and then averaged. Although rarely some pupils dilated to more than this value, the largest pupil diameter common to all eyes in our study was 6.0 mm, which was the value chosen for our analysis.

The aberrometer was specially configured to run using beta-software incorporating the new series of polynomials, $G(n,m)$ in addition to the Zernike polynomials. The acquired wavefront was decomposed with Zernike and LD/HD modes up to the 6th order and on the basis of a 6 mm pupil disk diameter centered on the first Purkinje image.

Fig. 3a-c display the statistical summaries of Zernike and LD/HD coefficients for the Normal, Keratoconus and post myopic LASIK eyes, respectively.

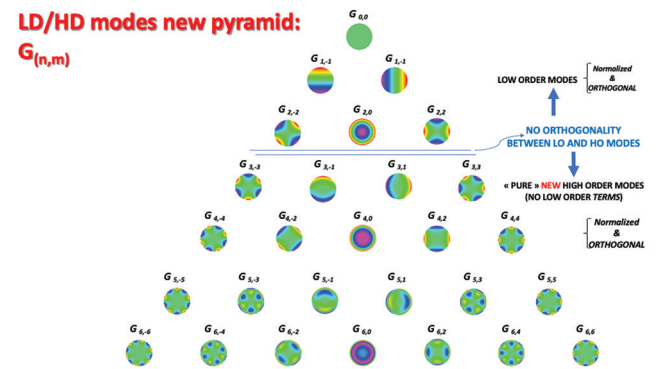


Figure 1: The LD/HD aberration classification proposes a clear distinction between low and high order aberrations. There is no orthogonality between the LO (Lower order) and HO (Higher order) subsets. However, orthogonality is maintained between the modes comprised in the low order and the high order space. The break in orthogonality echoes the clinical approach, which decouples the low (spectacle corrected) and high order aberrations

Inspection of these histograms indicates that most Zernike and LD/HD coefficients are distributed symmetrically around zero, as reported previously by Porter *et al.*^[28] However, for any individual eye the aberrations were rarely zero for any of the Zernike or LD/HD modes. The spherical aberration is a notable exception for normal and post myopic LASIK eyes, in which it is clearly biased toward positive values. Fourth order spherical aberration is larger in mean absolute RMS than any third-order mode among the three studied groups and the LD/HD coefficient is larger than that of its Zernike counterpart. This discrepancy is explained by the difference between the analytical structures of modes Z_4^0 and $G_4^{0,1,2,4}$ in brief, the presence of a defocus term (r^2) in the Z mode (4,0) expression causes an increase in the value of its normalization coefficient. This in turn induces a reduction in the value of the coefficient weighting that mode, compared to a mode pure in r^4 , for the same amount of phase error in r^4 . For that same analytical reason, LD/HD vertical and horizontal coma modes' coefficients have a larger amplitude than their Zernike counterparts. For normal eyes, when the coma aberration mode is pure in cubic r^3 terms as is the trefoil aberration, the magnitude of the coma aberration coefficients is greater within the radial 3 degree aberrations. This dominance of coma over trefoil is also observed for eyes with keratoconus as well as eyes operated for myopic LASIK. The use of high degree modes 3 and 4, devoid of low degree terms makes it possible to avoid minimizing certain coefficients and allows an unbiased comparison of the respective contributions of these modes for the high degree wavefront error.

Novel Clinical Applications of the LD/HD Polynomial Basis

Zernike versus LD/HD primary spherical aberration

Primary spherical aberration (SA) is one of the most significant higher order aberrations (HOAs) in the human eye.^[29] Most unaccommodated eyes have positive primary SA, in which the edge of the pupil is more myopic compared to the pupil center.

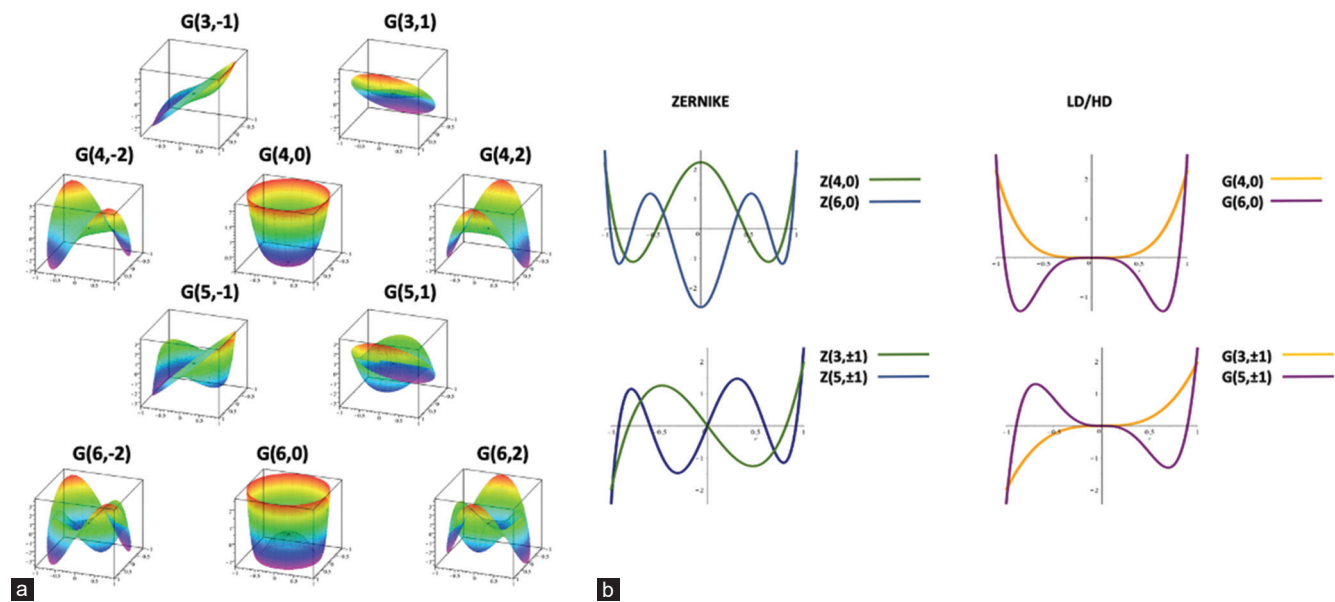


Figure 2: (a) Representation of the wavefront of each of the new higher order LD/HD modes $G(n,m)$ up to the 6th order, where n is the order of the aberration and m is the angular frequency. (b) Comparison between the cross-sectional profiles of some Zernike versus LD/HD mode (unit coefficient, normalized pupil). The absence of tilt and defocus terms in the analytical expression of the higher order LD/HD modes results in a flatter paraxial profile

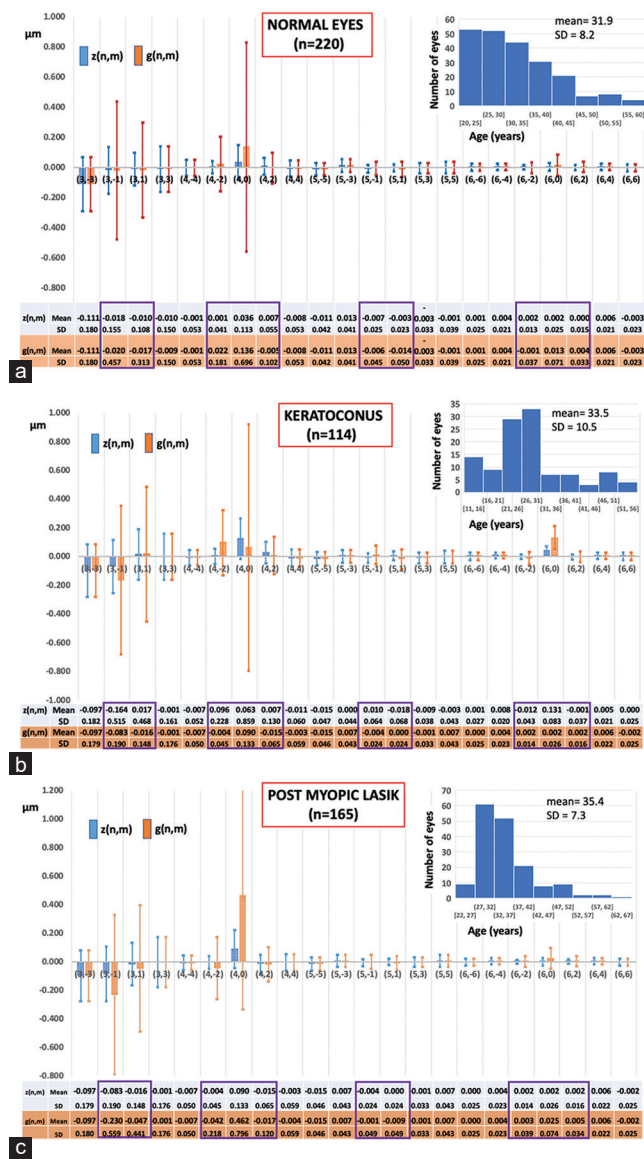


Figure 3: (a) normal eyes, (b) eyes with keratoconus, (c) eyes operated with myopic LASIK. Mean values of all Zernike and LD/HDS modes' coefficients in the specified population across a 6-mm pupil. The error bars represent plus and minus one standard deviation from the mean value. The values corresponding to the modes whose analytical expression differs between the Zernike and LD/HD decomposition methods are boxed. The frequency distribution of age of the patients may be seen in the inset figure

The Z_4^0 and G_4^0 modes and their respective analytical expression in polar coordinates are plotted on Fig. 4. The r^4 term is the distinguishing feature of the primary spherical aberration wavefront error. The G_4^0 mode is comparable to a Seidel polynomial, whereas Zernike SA has a lower order r^2 term embedded in this polynomial.

This anomaly has deleterious consequences for the clinical interpretation of the decomposition of a wavefront error or the expected effects of a personalized wavefront correction. If we consider a theoretical wavefront error limited to a pure 4th order spherical aberration (Z_4^0), part of it (the quadratic error r^2 it contains) can be corrected by spectacles, soft contact lenses, or conventional profiles of ablation.

Conversely, if a wavefront is limited to a pure error in r^4 (no low degree error), its reconstruction with a Zernike expansion will have a non-zero coefficient for the Z_4^0 mode, but the low mode degree Z_2^0 will also be assigned a non-zero coefficient of same sign to compensate for the term in degree that the latter contains. By adding positive Zernike SA to reconstruct a pure positive r^4 wavefront error, the objective refraction computed from the positive compensatory Zernike defocus coefficient will look myopic. This may cause confusion in some clinical situations and hamper the relevance of interpretation of the wavefront modifications. A clinical example illustrates this issue below.

Case 1

A 23-year-old man experiences mild halos at night after laser *in situ* keratomileusis (LASIK) for the correction of myopia (-3.00 diopters [D]). His left eye is emmetropic and has an uncorrected distance visual acuity of 20/15. The Zernike decomposition of the total wavefront on a 7.68 mm naturally dilated mesopic pupil in the left eye has a mixture of LOA and HOA coefficients, with the most prominent being defocus, despite the fact that this eye is emmetropic [Fig. 5a]. In the presence of increased amounts of positive spherical aberration, the magnitude of the coefficients of the second-degree modes is different between the Zernike and LDHD decompositions [Fig. 5b]. The sign of the defocus term is positive in the Zernike mode ($z_2^0 = 0.939$ microns) suggesting myopia and negative in the LDHD mode ($g_2^0 = -0.500$ microns). This Zernike predicted spherical equivalent is -1.12 D which contradicts the excellent uncorrected visual acuity. The positive Zernike defocus coefficient correlates with the need for compensating for the negative lower order term in r^2 embedded in the Z_4^0 mode. The LD/HD decomposition has negligible defocus, with no artificial reduction of the spherical aberration coefficient compared to its Zernike counterparts. This truly clinically significant HOA is highlighted within the novel decomposition.

The Snellen chart retinal image simulations can be obtained via convolutional techniques from the PSF function computed for the total wavefront aberrations [Fig. 6a], or its lower [Fig. 6b] versus higher order components [Fig. 6c] using the Zernike split between LO and HO components. The Snellen chart simulations suggest an exaggerated visual blur for the best spectacle corrected eye [Fig. 6b], and a best spherocylindrical visual acuity of less than 20/50 when just the higher order component of the Zernike expansion remains uncorrected [Fig. 6c]. When computed from the LD/HD wavefront split, the simulated Snellen chart retinal image for the uncorrected higher order component (HD) is in line with the patient's actual visual performance [Fig. 6d].

Zernike versus LD/HD for primary coma

The Fig. 2b plots the Zernike and the LD/HD primary coma modes and their respective equations.

As opposed to its counterparts of 3rd radial degree the Zernike primary trefoil $Z_3^{\pm 3}$, which is pure in r^3 , the Zernike primary coma contains a negative tilt term. This term makes Zernike coma orthogonal to the tilt of same azimuthal frequency ($m = 1$), whereas the different azimuthal frequency of trefoil ($m = 3$) makes it directly orthogonal to tilt. Hence, in an eye suffering from pure normalized Seidel-like coma aberration, the use of a Zernike coma mode to reconstruct such a wavefront would impose a non-null tilt coefficient to compensate for the tilt term present in the Zernike coma mode. This has detrimental consequences for the interpretation of the tilt amount, which is potentially interesting in the case of the expression of the corneal wavefront in special circumstances such as keratoconus, or the decentering of intraocular lenses or corrective photoablation in refractive surgery. Any increase in

the horizontal or vertical coma coefficients cause a concomitant increase of artifactual tilt in the low order wavefront component, whose magnitude is roughly equal to three times that of the Zernike coma coefficients.^[22,24] However, the presence of a pronounced tilt coefficient for a regular ocular wavefront examination should not be observed in clinical practice because it reflects the presence of a pronounced deviation in the direction of propagation of the wavefront with respect to that of the fixing axis, when these directions should in principle be parallel in the cases of coaxial fixation.

These interactions also have detrimental consequences to the titration of coma, with regards to the anatomical features involved in its genesis, as illustrated in the following case example.

Case 2

A 38-year-old male complains about slight monocular diplopia persisting after spectacle correction of his right eye. Seven years previously, he had a PRK (photorefractive keratectomy) in another centre. The immediate outcome on his right was the perception of an under correction and a reduction of the quality of vision. After correcting with the spectacles, the residual correction: -2.75 (-1 × 130°), the patient could draw how he perceived the 20/40 visual acuity “E” optotype. Fig. 7 shows the right eye axial corneal topography, suggestive of supero-nasal decentration of the myopic photoablation.

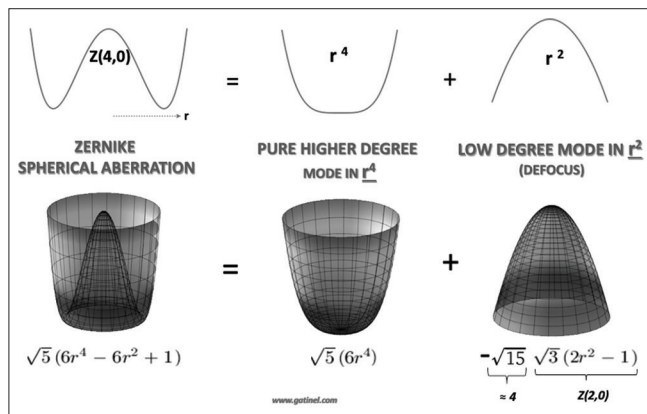


Figure 4: Decomposition of the Zernike 4th order spherical aberration Z40 mode into a component in r4 and a component in r2 which is equivalent to roughly 4 microns of Zernike defocus Z20

The Fig. 8a and b allow us to compare the Zernike versus LD/HD expansions’ coefficients for the total ocular and anterior corneal wavefront. Significant differences in the magnitude of the primary coma coefficients are obvious. Compared to those of the LD/HD expansion, the Zernike coma coefficients are minimized, whilst the Zernike tilt coefficients are artifactually increased. In addition, the low-order oblique astigmatism coefficient is higher in the LD/HD expansion ($g_2^{-2} = 1.789 \mu\text{m}$) than in the Zernike expansion ($z_2^{-2} = 1.003 \mu\text{m}$). This increase is due to the decoupling of the embedded low order astigmatism term present in the Z_4^{-2} mode. This low order astigmatism is transferred in the LD component of the LD/HD expansion.

The Fig. 9 allows a comparison of the predicted retinal images of the 20/40 “E” optotype for the respective higher order Zernike and LD/HD wavefront components and the patient’s drawing. When presented with the two simulated images, the patient acknowledged that the HD predicted simulation matched his subjective visual impression better.

The presence of low order astigmatism in the higher astigmatism Zernike modes causes an increased blur of the convoluted higher order Zernike component.

Zernike versus LD/HD for secondary astigmatism

As opposed to the $Z_4^{\pm 2}$ modes, the LD/HD equivalent of the high order astigmatism modes $G_4^{\pm 2}$ are pure in higher order terms [Fig. 2a]. Therefore, their shape is flat para-centrally, and has a monotonic phase variation in cross section.

As seen in the case 2 example, interactions between high and low order modes would occur for some pairs of Zernike modes such as secondary astigmatism $Z_4^{\pm 2}$ and primary astigmatism $Z_2^{\pm 2}$. These interactions could explain the discrepancies between anterior corneal astigmatism and refractive astigmatism when analyzed through Zernike polynomial decompositions in the context of topography-guided ablations.^[30] The following case illustrates the possible discrepancies arising from the interaction between the low order astigmatism within the low versus higher order wavefront component in the Zernike decomposition.

Case 3

A keratoconus pattern was discovered on the right eye corneal axial topography in a 24-year-old refractive surgery candidate [Fig. 10], with best corrected visual acuity of 20/15

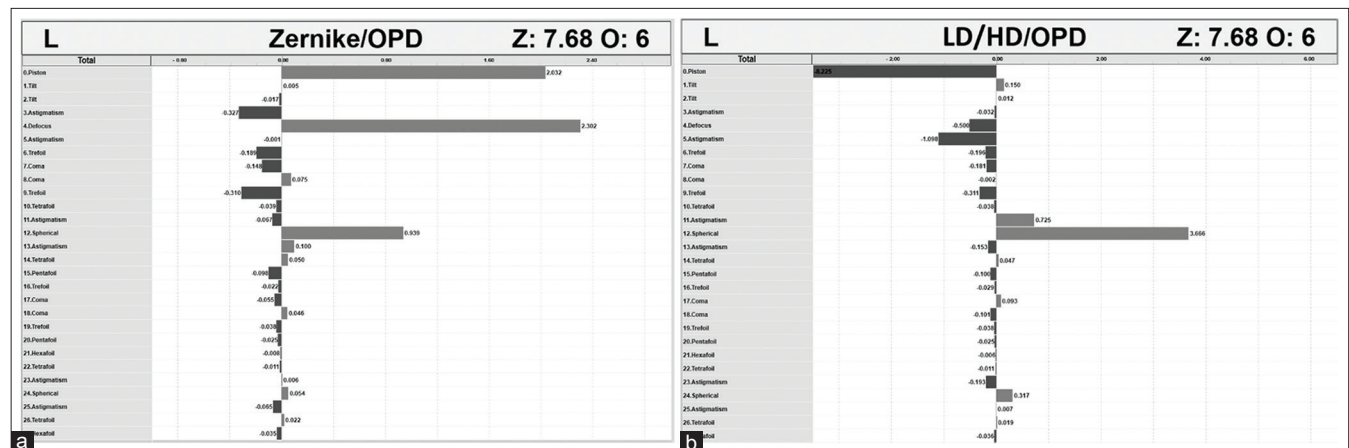


Figure 5: (a) Zernike decomposition of the ocular wavefront on a 7.68 mm pupil. The positive coefficient for defocus suggests the presence of a myopic residual refractive error. (b) LD/HD decomposition on a 7.68 mm pupil. The new coefficients of the LD/HD basis are obtained by adequately splitting the terms obtained from the lower and higher Zernike modes into their respective wavefront components. The wavefront error is dominated by positive spherical aberration. Note the dramatic reduction of the magnitude of the defocus coefficients and its sign inversion

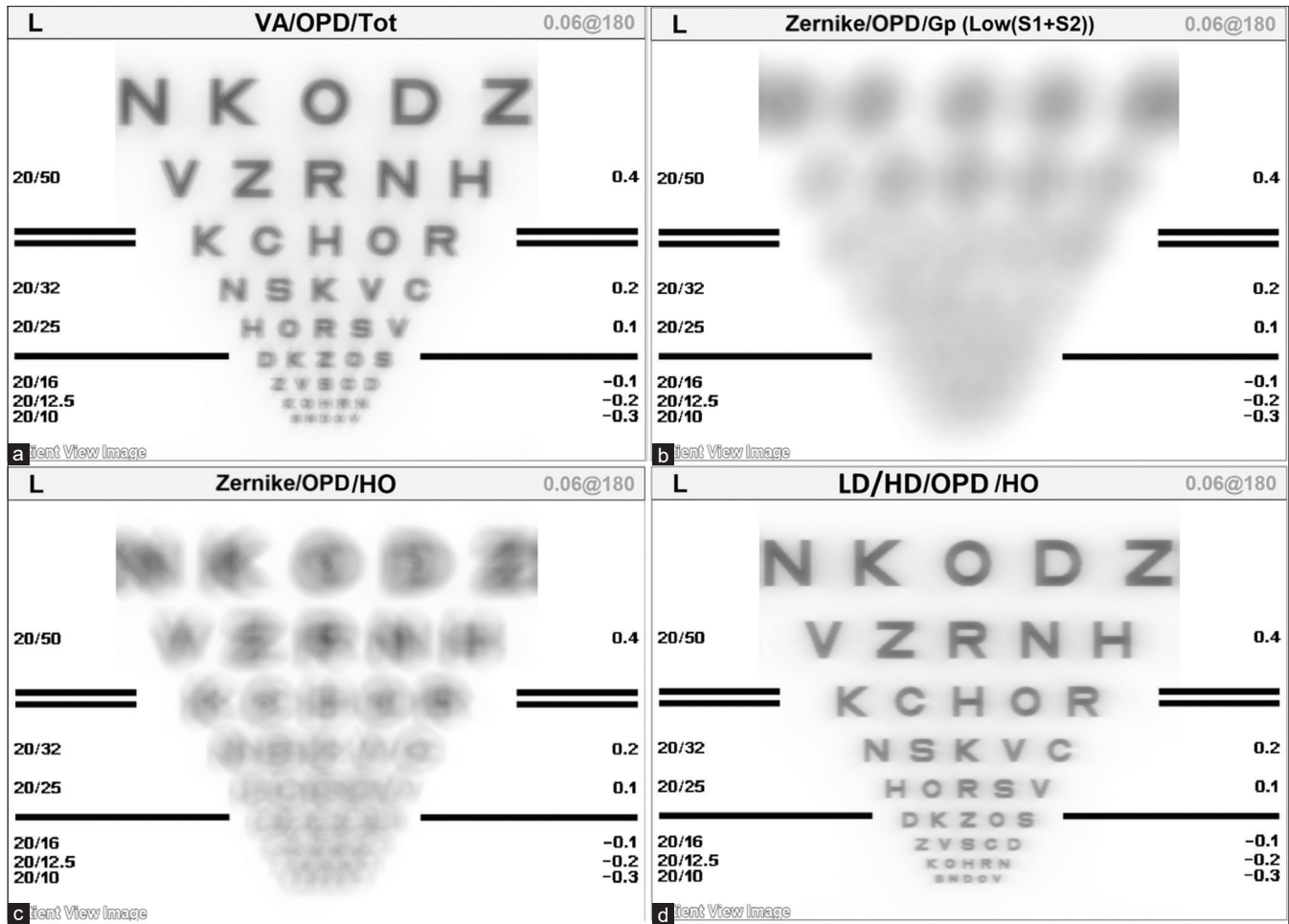


Figure 6: (a) Simulation of the retinal image of a Snellen chart of the uncorrected examined eye: optotypes corresponding to a resolution of 20/16 can be resolved (pupil diameter: 7.68 mm). (b) Simulation of the retinal image of a Snellen chart of the examined eye corrected for the Zernike high order only (7.68 mm pupil). The dramatic reduction in the resolution of optotype targets when correcting the higher order aberrations and leaving the eye with low order aberrations only is paradoxical and reflects the decoupling of Zernike’s defocus and the r2 term embedded in the Zernike Z40 mode. (c) Simulation of the retinal image of a Snellen chart of the examined eye corrected for the Zernike computed low order aberrations for the same pupil diameter (7.68 mm). There is a spectacular and paradoxical reduction in the resolution of Snellen’s target optotypes when only the high degree Zernike aberrations persist. This blur is caused by the unbalanced defocus term within the Z40 mode. (d) Simulation of the retinal image of a Snellen chart of the examined eye corrected for the LD order only (7.68 mm pupil). The comparison with the Fig. 5a shows that the higher order (HD) component causes a loss of the contrast of the simulated image, without major reduction in image resolution

with $-2.50/-0.50 \times 95^\circ$: The comparison between the wavefront analysis methods reveals a striking difference between the value of the vertical/horizontal astigmatism coefficients, which predict a “with the rule” orientation in the Zernike decomposition, and an “against the rule” orientation in the LD/HD decomposition [Fig. 11a]. This discrepancy involves the (clinically unwanted) presence of a low order astigmatism term within the Zernike higher order (secondary) astigmatism mode Z_4^2 [Fig. 11b]. In the Zernike decomposition, the value of the low order astigmatism coefficient is affected by the presence of HO astigmatism.

The central portion of the Zernike high order astigmatism is distorted by the presence of the low order astigmatism term. In this case, this undesirable low order astigmatism term, which has an “against the rule” orientation here, is subtracted from the low order component. Hence, this clinically relevant wavefront error, which would generate some against the rule low order astigmatism in the ocular refraction, is embedded in the secondary astigmatism mode, belonging to the higher order wavefront component.

Predicting Subjective Refraction

Uncorrected errors in refraction is a global burden and leading cause of moderate to severe visual impairment as highlighted by Honavar *et al.* recently with several secondary effects including social isolation, decrease in education and employment options leading to financial distress.^[31] In the Artificial intelligence era and the boom in literature relating to this,^[32-34] we explored the use of machine learning in order to validate the LD/HD polynomial decomposition with wavefront aberrometry in predicting subjective refraction.

Translating wavefront aberrometry calculations into a spherocylindrical spectacle prescription has been an evasive objective.^[35] The human eye is far from perfect with refraction greatly affected by HOAs. To date fitting this aberrated wavefront with different methods has given varying results.^[20,36,37]

We previously inferred that objective refraction calculated with the LD/HD polynomials could be more accurate.^[22] Though Thibos *et al.* had found that paraxial matching method could be used to predict spectacle correction,^[20] we

found that the machine learning technique using LD/HD decomposition method was more efficacious.^[38] This is due to the clinical need for a clear dissociation between the lower and higher wavefront aberration terms, as demonstrated in the clinical vignettes before, the presence of the low order terms in the higher order mode expressions leads to erroneous and misconstrued clinical interpretation of the results here.

There are of course limitations to this novel technique that can be explored in future studies. We have as yet to understand the full effects of chromatic aberrations on the clinical picture that patients describe. Also subjective refraction variability exists and this could add to the challenge of comparing any results against the current gold standard. Additionally, one must be aware that we have not concluded what is the correct weighting for different points within a pupil disk which contribute to the formation of the retinal image and may be more impactful for the subjective refraction.^[1]

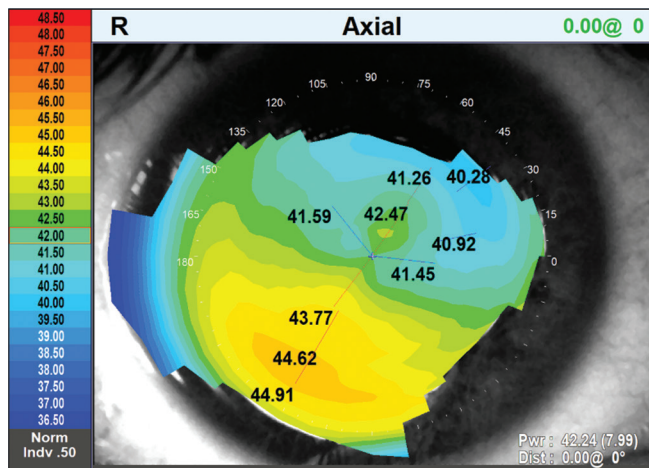


Figure 7: Postoperative axial topography (OPD scan III, Nidek, Gamagori, Japan) in an eye operated with myopic photorefractive keratectomy (PKR) suggestive of supero-nasal decentration of the photoablation

Customized Laser Corrections

Enhancing the benefits of a nomogram using Q factor modulation in presbyLASIK

Compensation for presbyopia with induction of multifocality of the cornea has been shown to give excellent visual outcomes.^[1,39-43] There should be cautious interpretation of the changes in defocus of the corneal wavefront using Zernike reconstruction following multifocal aspheric ablation, as the shift toward increased negative or positive asphericity may result in a significant negative variation of the z_2^0 wavefront coefficient accompanying the modulation of the z_4^0 coefficient. Investigating the effect of the LD/HD polynomial decomposition on prediction of effects with this novel technique demonstrates another valuable clinical application. We are currently studying the theoretical and clinical variation in lower and higher order aberrations between Zernike and LD/HD polynomial basis after customized presbyLASIK correction using Q factor modulation and spherical changes.

Enhancing the benefits for better topography-guided ablations

The presence of low-level terms in Zernike's spherical aberration mode also has consequences in the design of customized topographic corrections, such as those planned with the Contoura vision system (Alcon). To compensate for the spurious interactions between low and higher order Zernike modes, some surgeons recommend programming a defocus correction which will make the Zernike defocus coefficient c_2^0 (commonly designated as c4 in this context) equal to the value of the 4th order spherical aberration coefficient c_4^0 (designated as c12).^[44]

The use of a classification incurring a clear cut between low and higher order modes should alleviate the need of such adjustments and reduce the risk of redundant or spurious low degree correction

Conclusion

Currently, instruments such as the OPD scan III (Nidek, Gamagori, Japan) combine placido based corneal topography and whole eye aberrometry. As wavefront aberrometer

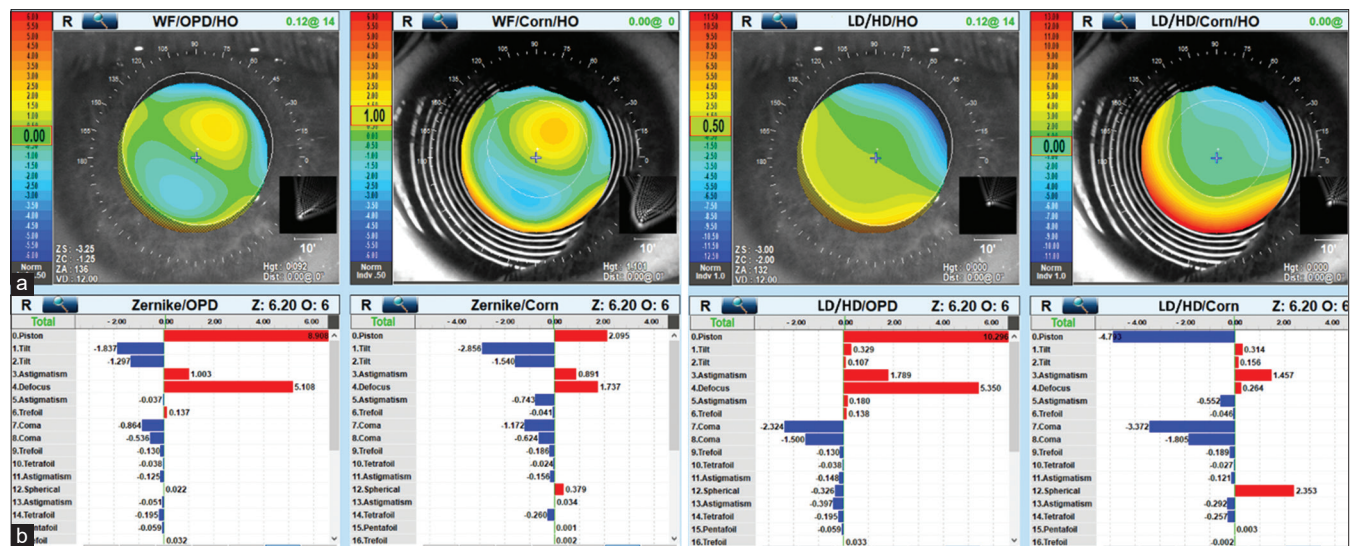


Figure 8: (a) Zernike higher order ocular (left) and corneal (right) wavefront components and the list of the first corresponding 16 Zernike coefficients (6.20 mm pupil). (b) LD/HD higher order ocular (left) and corneal (right) wavefront components and the list of the first corresponding 16 LD/HD coefficients (6.20 mm pupil)

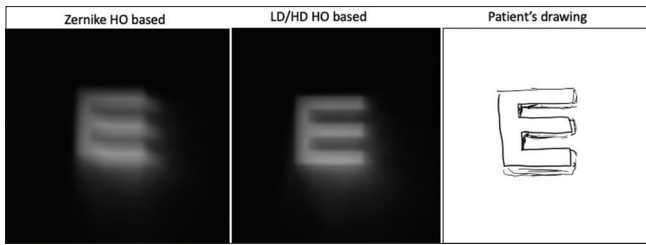


Figure 9: Comparison between the simulated retinal images of a 20/40 'E' letter optotype from the Higher order Zernike ocular wavefront component (left), the higher order LD/HD ocular wavefront component (center) and the patient's drawing (right)

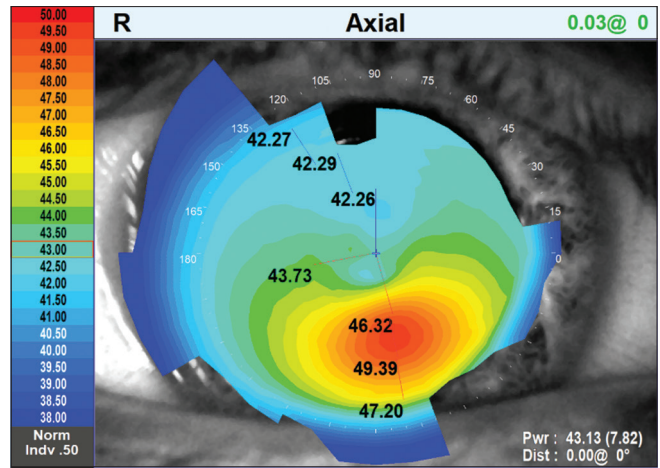


Figure 10: Axial corneal topography displaying marked inferior steepening suggestive of keratoconus

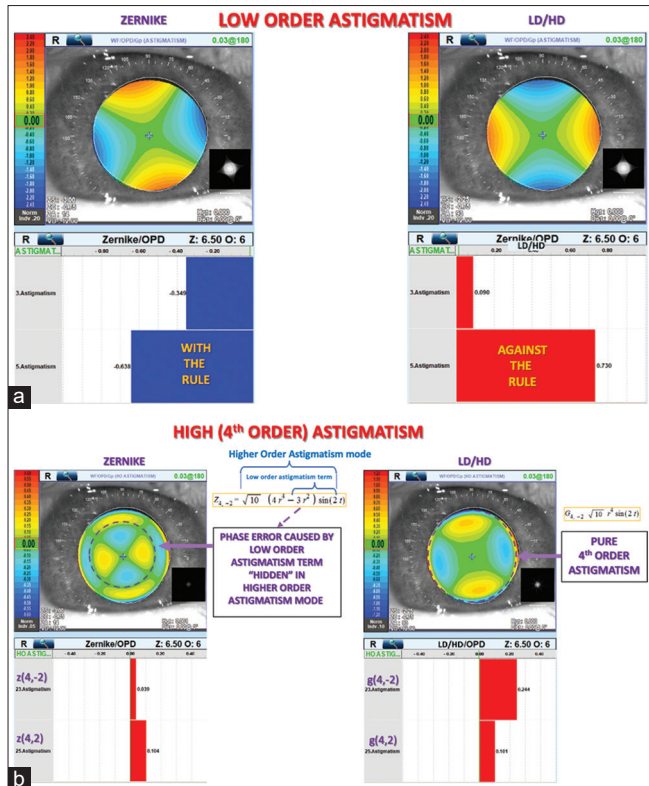


Figure 11: (a) Comparison of the shapes of the wavefront error restricted to low order astigmatism modes in the Zernike versus LD/HD decomposition methods. (b) Comparison of the shapes of the wavefront error restricted to higher order astigmatism modes in the Zernike versus LD/HD decomposition methods

technology advances we expect diagnostic tools to become more comprehensive with a multitude of functions including high resolution OCT with biometry as well as wavefront aberrometry. In addition to the ocular wavefront, the LD/HD decomposition method could be applied to the study of the corneal wavefront. It could induce a better correlation between apical curvature of the corneal diopter with the low-degree LD contingent of the wavefront on one side, and the parameters corresponding to variations in the peripheral curvature such as asphericity with certain modes of the high contingent HD degree on the other side.

In any case, the interpretation of the decomposition of the wavefront from a series of weighting coefficients of the particular aberration modes must be carried out with care. Each mode is fragmented information of a particular wavefront. It is not judicious to extract a particular aberration from the total

wavefront in order to predict its effect on the optical quality of the eye without taking into account the whole of the wavefront error.

Nevertheless, certain so-called low-degree aberrations are correctable with spectacles, and it is clinically important to be able to isolate them in a relevant way from the whole of the wavefront error. In this perspective, the possibilities offered by the LD/HD wavefront decomposition method are manifold. The absence of low degree terms in high degree modes should make it possible to better distinguish the influence on subjective refraction from high degree wavefront errors^[38] and make it possible to better appreciate the specific effect of high degree modes on the retinal image. The analytical homogeneity between the high degree modes makes it possible to better titrate the relative contribution of these modes to the high degree wavefront error. These applications are of potentially considerable importance in the field of personalized and multifocal surgical corrections.

The future direction of anterior segment and refractive surgery could benefit from personalized customizable results using LD/HD polynomial decomposition basis and machine learning.

Financial support and sponsorship

Nil.

Conflicts of interest

There are no conflicts of interest.

References

- Gatinel D. Chapter 5: Wavefront analysis. In: Azar DT, Gatinel D, Ghanem R, Taneri S, editors. Refractive Surgery. Elsevier; 2019. ISBN-13 9780323547697.
- Khurana. Theory and Practice of Optics and Refraction. Elsevier India; 2008.
- Maeda N. Clinical applications of wavefront aberrometry- A review. Clin Exp Ophthalmol 2009;37:118-29.
- Rozema JJ, Van Dyck DEM, Tassignon M-J. Clinical comparison of 6 aberrometers. Part 1: Technical specifications. J Cataract Refract Surg 2005;31:1114-27.
- Rozema JJ, Van Dyck DEM, Tassignon M-J. Clinical comparison of 6 aberrometers. Part 2: Statistical comparison in a test group. J Cataract Refract Surg 2006;32:33-44.
- Cade F, Cruzat A, Paschalis EI, Espirito Santo L, Pineda R. Analysis of four aberrometers for evaluating lower and higher order aberrations. PLoS One 2013;8:e54990.

7. Misra S, Cook W, McKelvie J, Wallace H. Comparison of higher order wavefront aberrations with four aberrometers. *Indian J Ophthalmol* 2019;67:1030-5.
8. Nguyen PM, Hirschschall N, Doeller B, Schuschitz S, Varsits R, Findl O. Comparability and reproducibility of four wavefront aberrometers for measuring lower and higher order aberrations in pseudophakic eyes. *Acta Ophthalmologica* 2015;93. doi: 10.1111/j.1755-3768.2015.0558.
9. Mahajan VN. Optical Imaging and Aberrations, Part III: Wavefront Analysis [Internet]. 2013. Available from: <https://spie.org/Publications/Book/927341>. [Last accessed January 2020].
10. Klyce SD, Karon MD, Smolek MK. Advantages and disadvantages of the Zernike expansion for representing wave aberration of the normal and aberrated eye. *J Refract Surg* 2004;20:S537-41.
11. Dai G-M. Wavefront Optics for Vision Correction. Society of Photo-Optical Instrumentation Engineers; SPIE press 2008.
12. Applegate RA, Sarver EJ, Khemsara V. Are all aberrations equal? *J Refract Surg* 2002;18:S556-62.
13. Applegate RA, Ballentine C, Gross H, Sarver EJ, Sarver CA. Visual acuity as a function of Zernike mode and level of root mean square error. *Optom Vis Sci* 2003;80:97-105.
14. Rossi EA, Roorda A. Is visual resolution after adaptive optics correction susceptible to perceptual learning? *J Vis* 2010;10:11.
15. Saad A, Gatinel D. Evaluation of total and corneal wavefront high order aberrations for the detection of forme fruste keratoconus. *Invest Ophthalmol Vis Sci* 2012;53:2978-92.
16. Saad A, Gatinel D. Topographic and tomographic properties of forme fruste keratoconus corneas. *Invest Ophthalmol Vis Sci* 2010;51:5546-55.
17. Chan C, Ang M, Saad A, Chua D, Mejia M, Lim L, *et al.* Validation of an objective scoring system for forme fruste keratoconus detection and post-LASIK ectasia risk assessment in Asian eyes. *Cornea* 2015;34:996-1004.
18. von Zernike F. Beugungstheorie des schneidenver-fahrens und seiner verbesserten form, der phasenkontrastmethode. *Physica* 1934;1:689-704.
19. Thibos LN, Applegate RA, Schwiegerling JT, Webb R; VSIA Standards Taskforce Members. Vision science and its applications. Standards for reporting the optical aberrations of eyes. *J Refract Surg* 2002;18:S652-60.
20. Thibos LN, Hong X, Bradley A, Applegate RA. Accuracy and precision of objective refraction from wavefront aberrations. *J Vis* 2004;4:329-51.
21. Cheng X, Bradley A, Ravikumar S, Thibos LN. Visual impact of Zernike and Seidel forms of monochromatic aberrations. *Optom Vis Sci* 2010;87:300-12.
22. Gatinel D, Rampat R, Dumas L, Malet J. An alternative wavefront reconstruction method for human eyes. *J Refract Surg* 2020;36:74-81.
23. Watson AB. Computing human optical point spread functions. *J Vis* 2015;15:26.
24. Gatinel D, Malet J, Dumas L. Polynomial decomposition method for ocular wavefront analysis. *J. Opt. Soc. Am.* 2018;24:235-45.
25. Gatinel D, Malet J, Dumas L. A new polynomial decomposition method for ocular wavefront analysis. *Opt Lett* 2018;2:6.
26. Muftuoglu O, Erdem U. Evaluation of internal refraction with the optical path difference scan. *Ophthalmology* 2008;115:57-66.
27. Buscemi P. Clinical applications of the OPD-Scan wavefront aberrometer/corneal topographer. *J Refract Surg* 2002;18(3 Suppl):S385-8.
28. Porter J, Guirao A, Cox IG, Williams DR. Monochromatic aberrations of the human eye in a large population. *J Opt Soc Am A Opt Image Sci Vis* 2001;18:1793-803.
29. Thibos LN, Bradley A, Hong X. A statistical model of the aberration structure of normal, well-corrected eyes. *Ophthalmic Physiol Opt* 2002;22:427-33.
30. Stulting RD, Durrie DS, Potvin RJ, Linn SH, Krueger RR, Lobanoff MC, *et al.* Topography-guided refractive astigmatism outcomes: Predictions comparing three different programming methods. *Clin Ophthalmol* 2020;14:1091-100.
31. Honavar SG. The burden of uncorrected refractive error. *Indian J Ophthalmol* 2019;67:577-8.
32. Varadarajan AV, Poplin R, Blumer K, Angermueller C, Ledsam J, Chopra R, *et al.* Deep learning for predicting refractive error from retinal fundus images. *Invest Ophthalmol Vis Sci* 2018;59:2861-8.
33. Libralao GL, Almeida OCP, Andre CPL. Classification of ophthalmologic images using an ensemble of classifiers. *Innov Appl Artif Intell* 2005;380-9.
34. Leube A, Leibig C, Ohlendorf A, Wahl S. Machine learning based predictions of subjective refractive errors of the human eye. Proceedings of the 12th International Joint Conference on Biomedical Engineering Systems and Technologies, Vol. 5. HEALTHINF; 2019. p. 199-205.
35. Applegate R, Atchison D, Bradley A, Bruce A, Collins M, Marsack J, *et al.* Wavefront refraction and correction. *Optom Vis Sci* 2014;91:1154-5.
36. Smolek MK, Klyce SD. Zernike polynomial fitting fails to represent all visually significant corneal aberrations. *Invest Ophthalmol Vis Sci* 2003;44:4676-81.
37. Kilintari M, Pallikaris A, Tsiklis N, Ginis HS. Evaluation of image quality metrics for the prediction of subjective best focus. *Optom Vis Sci* 2010;87:183-9.
38. Rampat R, Debellemanière G, Malet J, Gatinel D. Using artificial intelligence and novel polynomials to predict subjective refraction. *Sci Rep* 2020;10:8565.
39. Courtin R, Saad A, Grise-Dulac A, Guilbert E, Gatinel D. Changes to corneal aberrations and vision after monovision in patients with hyperopia after using a customized aspheric ablation profile to increase corneal asphericity (Q-factor). *J Refract Surg* 2016;32:734-41.
40. Jain S, Arora I, Azar DT. Success of monovision in presbyopes: Review of the literature and potential applications to refractive surgery. *Surv Ophthalmol* 1996;40:491-9.
41. Ryan A, O'Keefe M. Corneal approach to hyperopic presbyopia treatment: Six-month outcomes of a new multifocal excimer laser *in situ* keratomileusis procedure. *J Cataract Refract Surg* 2013;39:1226-33.
42. Alió JL, Chaubard JJ, Caliz A, Sala E, Patel S. Correction of presbyopia by technovision central multifocal LASIK (presbyLASIK). *J Refract Surg* 2006;22:453-60.
43. Leray B, Cassagne M, Soler V, Villegas EA, Triozon C, Perez GM, *et al.* Relationship between induced spherical aberration and depth of focus after hyperopic LASIK in presbyopic patients. *Ophthalmology* 2015;122:233-43.
44. Motwani M. The use of WaveLight® Contoura to create a uniform cornea: The LYRA Protocol. Part 3: The results of 50 treated eyes. *Clin Ophthalmol* 2017;11:915-21.